

SIMULATION OF THE AERODYNAMIC CHARACTERISTICS OF CAR SIDE MIRRORS

Paulo Eduardo Batista de Mello, pmello@fei.edu.br

Bruno Gimenez Fernandes, brunogimenez.carpediem@gmail.com

FEI – Fundação Educacional Inaciana

Av. Humberto de Alencar Castelo Branco, 3872 – São Bernardo do Campo – SP – Brazil – 01525-000

Abstract. *The aerodynamic characteristics of a car side mirror are investigated using CFD simulations. Due to the shape of car side mirrors, one turbulent wake is formed behind these bodies. The nature of this wake is greatly influenced by the geometry of the body and characteristics of the flow. The determination of the drag in the car side mirror is not trivial. The literature reports that the use of standard RANS models fail to reproduce experimental measurements, particularly the drag. The present paper presents results for the turbulent simulation of the flow around one car side mirror, using the SAS model (Scale-adaptive-simulation), capable of obtaining LES-like results, but using significantly less computational resources. The drag and frequency of the vortex generated in the wake are presented and compared to experimental results from the literature. The influence of one geometric parameter over the drag is investigated.*

Keywords: *drag, CFD, car side mirror, turbulent wake*

1. INTRODUCTION

Every CFD simulation should be conducted with one particular purpose. The purpose of simulating the aerodynamic flow around a car side mirror is to produce important information during design stage: the drag and its fluctuation; the lift and its fluctuation; the frequency of these fluctuations. The drag and the lift are of obvious importance as it has impact over the aerodynamic behavior of the vehicle. The problems that arise from the fluctuating behavior of the drag and lift are not so obvious. The magnitude of these fluctuations is not enough to cause structural problems related to fatigue, but the frequency spectrum of these fluctuations is one important information that must be considered during the design stage. The mirror itself, which is located inside one aerodynamic cover, can present excessive vibration if its natural frequency is tuned with the vortex shedding formed in the wake.

Rind and Hu (2007) present one experimental and numerical investigation of the aerodynamic flow around one lateral side mirror. They have investigated the flow over one constant two dimensional section ($L/D=6$), where L is the dimension in the axial direction and D the diameter, with variations in one geometrical parameter: the position of the mirror inside the aerodynamic cover. The Reynolds range considered in their work is between 1.1×10^5 and 2.6×10^6 . The flow pattern was evaluated qualitatively using PIV measurements. Hot wire anemometry was used to measure the energy spectra in one point in the wake, in order to obtain the vortex shedding frequency. Rind and Hu (2007) observed that the variation in the position of the mirror inside the aerodynamic cover did not affect the vortex shedding frequency. They have observed drag reduction around 11% for one particular positioning of the mirror inside the aerodynamic cover. Finally, they conducted also some CFD simulations, using one two dimensional grid, and different RANS (Reynolds-averaged Navier-Stokes) turbulence models available in the Fluent CFD code (steady state simulations). The RANS simulations were not capable of reproducing the experimental results and predicted drag coefficients 85% lower than the experiment.

The limitation of RANS models in producing satisfactory drag predictions for the flow around bluff bodies is notorious. LES (Large eddy simulation) and DES (Detached eddy simulation) are the common choice for this kind of simulations. Oliveira et al (2005) conducted 2D simulations of the flow over circular cylinders comparing the performance of these two different turbulence models (DES and LES). Their results show that DES simulations produced better results than URANS (unsteady RANS), but did dumped the fluctuations in the drag and lift coefficients if compared to LES results. Simulations with LES produced mean drag estimates more close to experimental results, but the best prediction for the Strouhal number was obtained with DES simulations.

The main benefit obtained with the DES method, if compared to LES, is the reduction in computational cost, because DES is a hybrid LES/RANS method. Noletto and Brasil Junior (2005) have used the DES model to conduct 3D simulations of the flow around a finite cylinder mounted on a flat plate, with $L/D \cong 4$. With a time step of 10^{-4} s, that is typical for the proper characterization of the transient vortex shedding, they have conducted DES with 100s of total time. Comparison of the simulations with experimental results has shown satisfactory agreement.

DES is not the only hybrid LES/RANS method available. One very complete review of hybrid LES/RANS methods is presented by Fröhlich and Terzi (2008). In this review, the details of DES implementation are presented. Enhancements introduced in the DES method during the last years are also discussed. New methods, classified by the authors as “second generation URANS” are presented and discussed, between them, the SAS (scale-adaptive simulation) developed by Menter and Egorov (2008).

Fröhlich and Terzi (2008) report some advantages of the SAS method, if compared to LES and DES. One of these advantages is the simplicity with which it can be implemented into an existing RANS solver. Another one is that the user is not requested to specify model parameters or to follow a rigorous mesh generation procedure. In the case the mesh generated is not sufficiently refined to resolve turbulent fluctuations, the method tends to produce RANS like solutions. This behavior is desired for industrial applications.

The most updated version of SAS model is presented by Egorov and Menter (2008). The authors implemented the SST-SAS in Ansys CFX and describe de SAS model as a new class of the URANS models, capable of adjusting the length scale to the local flow inhomogeneities. The model behaves like RANS models in stationary regions of the flow, independently of grid refinement. In separation zones, where transient instabilities take place, the model reduces the eddy viscosity accordingly, which permits to resolve turbulent spectrum down to the grid limit.

Egorov and Menter (2008) present the results obtained with the SAS method compared to experiments, for many different flows, in order to conduct one validation of the method. The validation presented includes one aero-acoustic simulation. The authors report good agreement between SAS and experiments. Davidson (2006) presents one comparison of the results produced by SST-SAS and SST-URANS. For one particular geometry simulated (asymmetric diffuser with opening angle at 10°) SAS have produced poorer results if compared to URANS. It is not clear if the version of the model implemented by Davidson (2006) is the most recent one. This could be one reason for the poor results obtained.

The objective of the present work is to evaluate a numerical model for the simulation of the transient flow around a blunt body, representing a car side mirror. As a result it is expected to obtain the drag and lift coefficients and the frequency of fluctuations in these forces, in the form of Strouhal number. These important parameters could be used to prevent vibration issues in the design of car side mirrors, avoiding the possibility of resonance and image blurring effects in the mirror. The numerical results are compared with experimental results from literature.

2. NUMERICAL MODEL

The simulations conducted in the present work are transient, two-dimensional and at constant properties. Differential equations for the conservation of mass and momentum are presented by eq. 1 and 2.

$$\nabla \cdot (\rho U) = 0 \quad (1)$$

$$\frac{\partial \rho U}{\partial t} + \nabla \cdot (\rho U \otimes U) = -\nabla p + \nabla \cdot \left[(\mu + \mu_t) (\nabla U + (\nabla U)^T) \right] \quad (2)$$

where U is the velocity, t the time, p the pressure, ρ the density of the fluid, μ the dynamic viscosity and μ_t the turbulent viscosity. The turbulent viscosity is dependant on modeling. The turbulence model used in the present work is the SST-SAS. The SST (shear stress transport) model was first introduced by Menter (1994), and has received some updates during the time to improve its capabilities, as described by Versteeg and Malalasekera (2007). Basically, it is a hybrid between k - ω and k - ε , switching between these two models where they present better performance: k - ω in the near-wall region and k - ε in the fully turbulent region. The turbulent viscosity used in the SST is given by eq. 3.

$$\mu_t = \frac{\rho a_1 k}{\max(a_1 \omega; S F_2)} \quad (3)$$

where a_1 is a constant, k the turbulence kinetic energy, ω the turbulence eddy frequency, F_2 a blending function and S one invariant measure of the strain rate. Note that turbulent viscosity calculated by eq. 3 is limited in regions with high strain rate: adverse pressure gradients and wakes.

Two differential equations are necessary to provide k and ω values used in eq. 3. The equations in the form used by standard SST are given by eq. 4 and 5.

$$\frac{\partial \rho k}{\partial t} + \nabla \cdot (\rho U k) = \nabla \cdot \left[\left(\mu + \frac{\mu_t}{\sigma_k} \right) \nabla k \right] + P_k - \rho c_\mu k \omega \quad (4)$$

$$\frac{\partial \rho \omega}{\partial t} + \nabla \cdot (\rho U \omega) = \nabla \cdot \left[\left(\mu + \frac{\mu_t}{\sigma_\omega} \right) \nabla \omega \right] + (1 - F_1) \frac{2\rho}{\sigma_{\omega 2} \omega} \nabla k \nabla \omega + \alpha \frac{\omega}{k} P_k - \rho \beta \omega^2 \quad (5)$$

where P_k is the turbulent production rate and F_1 a blending function. The values of variables σ_k , σ_ω , $\sigma_{\omega 2}$, α and β in eq. 4 and 5 are evaluated from linear interpolation, in order to reproduce the constants of standard k- ϵ or k- ω depending on the value of the blending function F_1 . The most updated model can be found in Menter et al. (2003).

The SAS model used in the present work is implemented with a modification introduced in the SST model. It is described in detail by Egorov and Menter (2008). The modification is introduced in the conservation equation for ω eq. 5, through a source term. The effect of this source term is to reduce the turbulent viscosity avoiding the damping effect over transient instabilities. The source term is given by eq. 6.

$$Q_{SAS} = \max \left[\rho \zeta_2 \kappa S^2 \left(\frac{L_S}{L_{vK}} \right)^2 - C \frac{2\rho k}{\sigma_\phi} \max \left(\frac{|\nabla \omega|^2}{\omega^2}, \frac{|\nabla k|^2}{k^2} \right), 0 \right] \quad (6)$$

Some constants present in eq. 6 assume the following values: $\sigma_\phi=2/3$; $\zeta_2=3.51$, $C=2$ and $\kappa=0.4$. The von Karman length scale L_{vK} and the modeled length scale L_S , both present in eq. 6, are given by eq. 7 and 8 respectively.

$$L_{vK} = \max \left(\frac{\kappa S}{|\nabla^2 U|}, C_S \sqrt{\frac{\kappa \zeta_2}{((\beta/c_\mu) - \alpha)}} \cdot \Omega_{CV}^{1/3} \right) \quad (7)$$

$$L_S = \frac{\sqrt{k}}{c_\mu^{1/4} \omega} \quad (8)$$

Where Ω_{CV} is the control volume size and C_S one constant that is dependant on the discretization scheme and assumes the value 0.11 in CFX code, as described by Egorov and Menter (2008).

2.1. Boundary Conditions

The boundary conditions are summarized in fig. 1. At the inlet, uniform velocity and turbulence intensity of 5% were set. The other boundaries use the opening condition, equivalent to specify a constant relative pressure, which permits the flow to enter and exit the domain. The surface of the blunt body is also a boundary of the calculation domain: at this position the no slip condition is set (zero velocity at the wall). The results presented in sections 3.1 and 3.2 use similar boundary conditions. Only the velocity value at the inlet is changed.

The dimensions of the domain are 4250 mm long (main flow direction) and 2125 mm high (perpendicular to main flow). The blunt body is positioned midway in the vertical direction and 1360 mm from the inlet. The diameter of the blunt body is 85 mm.

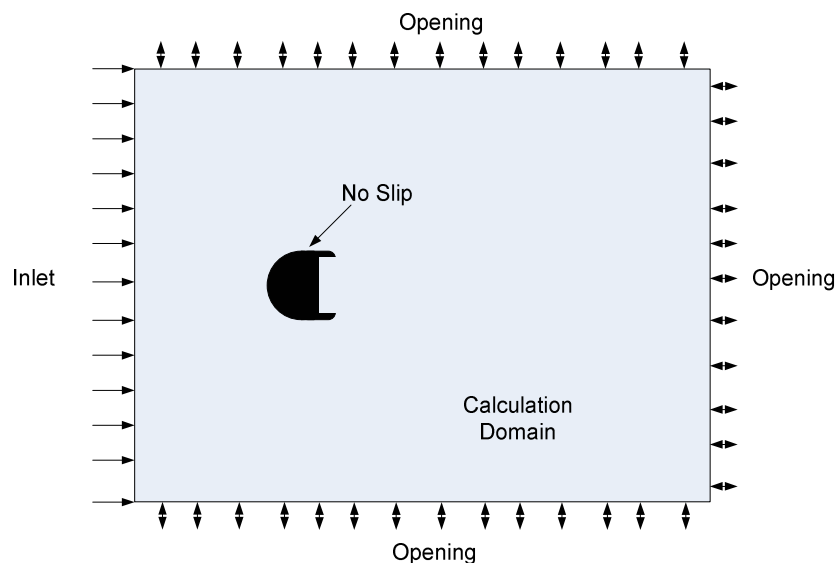


Figure 1. Domain used for the two-dimensional simulation and boundary conditions. (out of scale)

3. RESULTS

The code used for the simulations, CFX version 11, has the SST-SAS turbulence model implemented. It is a well known commercial code, and detailed explanation about how it works is unnecessary, but it does present many different optional models. Only some of the optional models are commented herein. For the discretisation of the advection terms of the differential equations, the high resolution scheme is used. This scheme tends to the CDS – central differencing scheme – in regions with small gradients. Near discontinuities, the scheme switches to first order, to guarantee a bounded solution. Other schemes are also available, but were not used in the present work.

The results presented are divided in two sections. Section 3.1 presents one comparison with the simulation results from literature, conducted by Oliveira et al. (2005), obtained with LES and DES models, using two dimensional grids. Section 3.2 presents the simulations of a two dimensional car side mirror. It was investigated the capability to predict the drag reduction observed in experimental tests conducted by Rind and Hu (2007).

3.1. Two dimensional flow over circular cylinder

In order to compare the results produced by the SAS model with similar simulations from the literature, simulations of the flow past circular cylinders were conducted. One calculation domain with the same dimensions reported by Oliveira et al. (2005) was used. One grid independence test was conducted. Most part of the grid is composed by triangular prisms, but rectangular prisms are used in the cylinder walls.

The simulation was conducted for Reynolds 10^4 . The same behavior as LES and DES simulations conducted by Oliveira et al (2005) is obtained with the SAS model. Figure 2 presents the temporal evolution of the drag and lift coefficients. One time step of 2×10^{-3} s was used in the simulation.

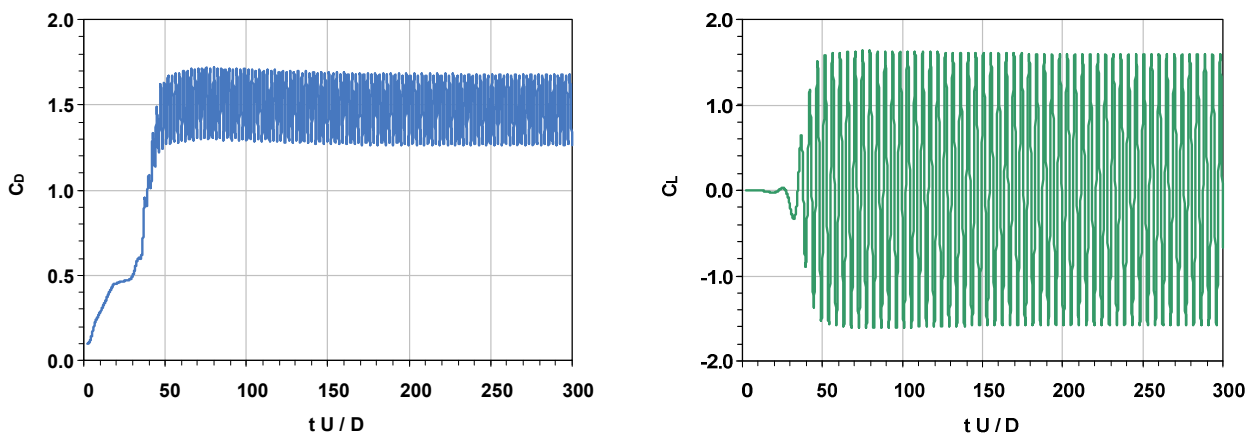


Figure 2. Temporal evolution of the drag (a) and lift (b) coefficients: two dimensional circular cylinder.

Oliveira et al (2005) have made a very complete discussion of their results, comparing the different turbulence models (LES, DES and URANS) with experimental results from literature, for a range of Reynolds numbers. Here, it is presented a brief comparison, for $Re=10^4$ only, including the results obtained with the two dimensional simulations using the SAS model. Two parameters are considered: the mean drag coefficient and the Strouhal number. This comparison is summarized in table 1.

Table 1. Mean drag coefficient (C_D) and Strouhal number (St): comparison of the SAS results with other models and experiments. $Re=10^4$.

	Simulation with turbulence model				Experiments		
	URANS ⁽¹⁾	DES ⁽¹⁾	LES ⁽¹⁾	SAS ⁽²⁾	White, 1991	Schlichting, 1979	Zdravkovich, 1997 ⁽¹⁾
C_D	0.8782	0.9840	1.2203	1.487	1.091	1.139	—
St	0.1877	0.2125	0.2507	0.209	—	—	0.2117

⁽¹⁾: Oliveira et al (2005)

⁽²⁾: Present work

The comparison of the results have shown that the SAS model was able to predict the frequency of vortex shedding with excellent accuracy, but was not able to produce a good estimate to the mean drag coefficient. Figure 1 shows that the lift fluctuations predicted by the SAS model is very intense. The RMS of C_L' obtained with SAS is 1.022, while for

C_D' is 0.127. Oliveira et al (2005) did not present these parameters, but inspecting the graphs presented in their work, it is possible to affirm that SAS is over predicting fluctuations, if compared to the other turbulence models.

One possible cause for the bad performance of SAS related to the prediction of the drag is the use of two dimensional simulation. Oliveira et al. (2005) states that three dimensional effects should be more intense after the drag crisis ($Re > 2 \times 10^5$). However, Egorov and Menter (2008) suggest that even for two dimensional geometry, the SAS model should be used only with three dimensional simulations.

3.2. Two dimensional flow over car side mirror

Rind and Hu (2007) have conducted experimental tests in wind a tunnel, using a two dimensional bluff body that represents a car side mirror assembly. The cross section of the bluff body is shown in fig. 3. The position of the mirror inside the frame is varied in order to evaluate this influence over the aerodynamic behavior of the assembly. The dimension λ represented in fig. 3 is given by eq. 9.

$$\lambda = L_M \cdot D \tag{9}$$

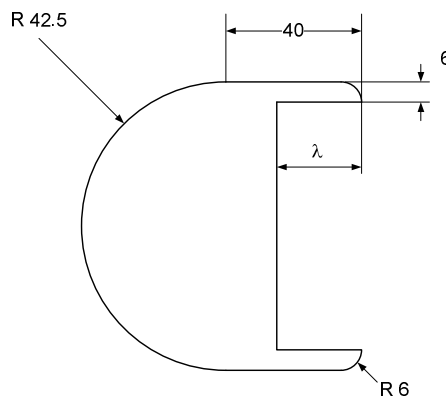


Figure 3. Cross section of the two dimensional car side mirror. (dimensions in millimeters)

Where λ is the distance from the mirror (flat shape) to the most external part of the cover.

Rind and Hu (2007) observed experimentally a drag reduction in the two-dimensional car side mirror when the L_M non-dimensional parameter is increased. The drag reduction is proportional to the increase in L_M . The range of Reynolds number investigated experimentally is from 1.1×10^5 to 2.6×10^5 , and the range of L_M from 0.0 to 0.175. The maximum drag reduction is observed for $L_M=0.175$ and $Re=2.6 \times 10^5$ (11% of drag reduction).

In the present work, it was investigated the capability of the SAS turbulence model to predict the drag reduction observed experimentally by Rind and Hu (2007). Three two dimensional simulations were conducted, for a fixed Reynolds number of 1.1×10^5 , with three different values of L_M : 0.0, 0.105 and 0.175. Figure 3 shows the typical temporal evolution of the drag and lift coefficients, for the case with $L_M=0.105$. It was necessary to increase the simulation total time in order to obtain mean values. For these simulations, the total non-dimensional time tU/D was set around 500.

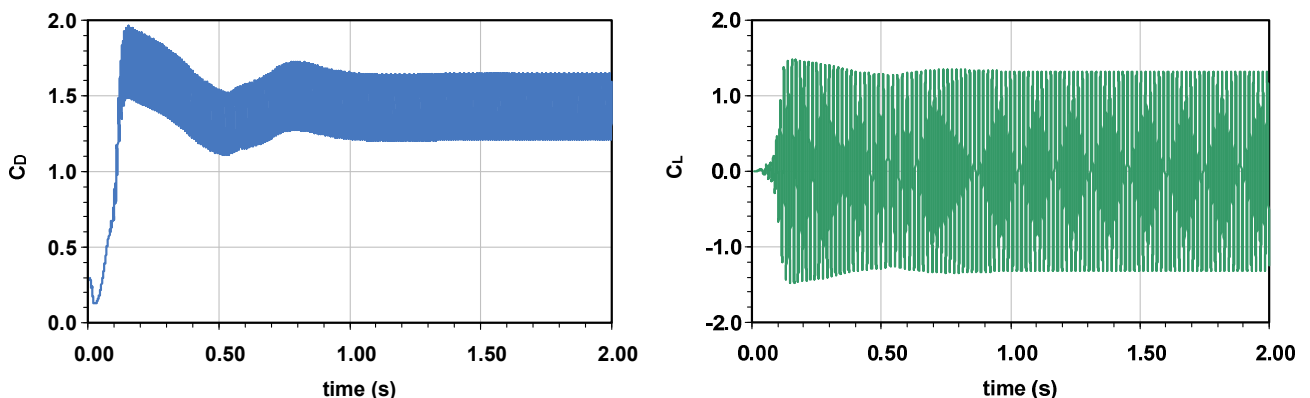


Figure 4. Temporal evolution of the drag (a) and lift (b) coefficients. Two dimensional car side mirror.
 $Re=1.1 \times 10^5$; $L_M=0.105$.

Figure 5 presents the vorticity distribution in the wake formed downstream of the car side mirror. The behavior of the flow is the same observed for the case of circular cylinders. The modification in the geometry, for the cases with $L_M > 0$, don't produce modifications in this behavior.

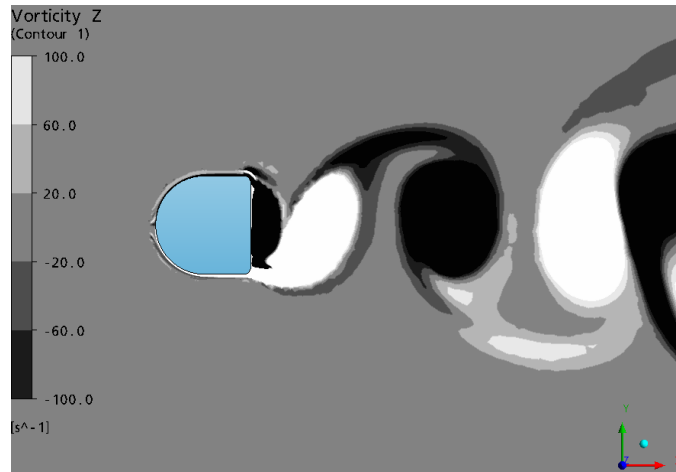


Figure 5. Vorticity distribution in the wake of the two-dimensional car side mirror.

Table 2 summarizes the results obtained with this set of simulations and presents the comparison with the experimental tests of Rind and Hu (2007). One direct comparison with the drag coefficients is not possible since the experiments were obtained for one aspect ratio $L/D \sim 6$ (L is the dimension in the axial direction and D the diameter of the cylinder). This aspect ratio is too small to compare with the two-dimensional case. Considering this, tab. 2 shows only the influence of distance L_M (which determines the position of the mirror inside its cover) on the drag coefficient.

Table 2. Mean drag coefficient (C_D) and Strouhal number (St): comparison of the SAS results with experiments performed by Rind and Hu (2007). $Re=1.1 \times 10^5$.

L_M	Modification on drag		Strouhal number	
	Experiments ⁽¹⁾	SAS turbulence model ⁽²⁾	Experiments ⁽¹⁾	SAS turbulence model ⁽²⁾
0.000	Reference; $C_D=0.82$	Reference; $C_D=1.37$	0.26	0.252
0.105	- 8%; $C_D=0.75$	+5.6% $C_D=1.45$	0.26	0.237
0.175	- 10%; $C_D=0.73$	+2.6% $C_D=1.41$	0.26	0.251

(1): Rind and Hu (2007)

(2): Two dimensional simulations

Despite the good concordance obtained for the frequency in the vortex shedding, in the form of Strouhal number, the results obtained with the two dimensional simulations using the SAS model were not able to predict the drag reduction. The drag coefficients C_D can't be compared directly due to different aspect ratios (L/D). The simulations predicted increase in the drag, when the L_M parameter is increased, that is contrary to experimental observations.

Similar simulations performed by Egorov and Menter (2008) using the SST-SAS turbulence model for the flow over NACA 0021 airfoil have shown excellent agreement with experiments, but the simulations performed by them use three dimensional domains. Apparently, it is essential to include three dimensional effects in the simulations of this kind of flows.

4. CONCLUSIONS

The results obtained with two dimensional simulations have shown reasonable agreement with experimental data. The Strouhal number predicted is very close to experimental measurements. The simulations conducted were not able to predict the drag reduction obtained with geometry modifications introduced in the car side mirror reported by the experiments of Rind and Hu (2007).

The disagreement between numerical results and experiments may be attributed to the limitation introduced by two dimensional simulations and not to the turbulence model used. The results obtained with SST-SAS model is very close to results obtained with LES and DES, found in literature.

Despite the apparent two dimensionality of the problem considered herein, it is known that, even for this kind of flow, three dimensional effects are dominant in turbulence. It is believed that new investigations should be performed with three dimensional simulations in order to improve these preliminary results.

5. REFERENCES

- Davidson, L., 2006, "Evaluation of the SST-SAS model: channel flow, asymmetric diffuser and axi-symmetric hill", European Conference on Computational Fluid Dynamics, ECCOMAS CFD 2006, pp. 1-20.
- Egorov, Y., Menter, F., 2008, "Development and application of SST-SAS turbulence model in the DESIDER project", Adv. In Hybrid RANS-LES modelling, Springer, pp. 261-270.
- Fröhlich, J., Terzi, D., 2008, "Hybrid LES/RANS methods for the simulation of turbulent flows", Progress in Aerospace Sciences, Vol. 44, pp. 349-377.
- Maliska, C. R., 2006, "Transferência de calor e mecânica dos fluidos computacional", LTC, 2nd ed., 453 p.
- Menter, F. R., 1994, "Two-Equation Eddy-Viscosity Turbulence Models for Engineering Applications", AIAA Journal, Vol.32, No. 8, pp. 1598-1605.
- Menter, F. R., 2003, "Ten years of industrial experience with the SST turbulence model", Turbulence, Heat and Mass Transfer, N.4.
- Noletto, L. G., Brasil Junior, A. C. P., 2005, "DES simulation of a finite cylinder mounted on a flat plate", 18th International Congress of Mechanical Engineering.
- Oliveira, J. E. S., Silva, A. L. L., Souza, F. J., Silveira Neto, A., 2005, "Numerical simulation of high Reynolds number flows over circular cylinders using the immersed boundary method", 18th International Congress of Mechanical Engineering.
- Rind, E., Hu, Z. W., 2007, "Aerodynamics of F1 car side mirror", Report No. AFM-07/06, University of Southampton.
- Versteeg, H. K., Malalasekera, W., 2007, "An introduction to computational fluid dynamics: the finite volume method", Pearson, 2nd ed., 503 p.

6. RESPONSIBILITY NOTICE

The authors are the only responsible for the printed material included in this paper.

7. ACNOWLEDGEMENTS

The authors would like to thank FEI – Fundação Educacional Inaciana – for the support.